

HENRY

Hydraulic Engineering Repository

Ein Service der Bundesanstalt für Wasserbau

Conference Paper, Published Version

Putzar, B.; Malcherek, A.

Numerical Prediction of Ripple Dimensions and Related Roughness for Tidal Environments

Zur Verfügung gestellt in Kooperation mit/Provided in Cooperation with:
Kuratorium für Forschung im Küsteningenieurwesen (KFKI)

Verfügbar unter/Available at: <https://hdl.handle.net/20.500.11970/109851>

Vorgeschlagene Zitierweise/Suggested citation:

Putzar, B.; Malcherek, A. (2010): Numerical Prediction of Ripple Dimensions and Related Roughness for Tidal Environments. In: Sundar, V.; Srinivasan, K.; Murali, K.; Sudheer, K.P. (Hg.): ICHE 2010. Proceedings of the 9th International Conference on Hydro-Science & Engineering, August 2-5, 2010, Chennai, India. Chennai: Indian Institute of Technology Madras.

Standardnutzungsbedingungen/Terms of Use:

Die Dokumente in HENRY stehen unter der Creative Commons Lizenz CC BY 4.0, sofern keine abweichenden Nutzungsbedingungen getroffen wurden. Damit ist sowohl die kommerzielle Nutzung als auch das Teilen, die Weiterbearbeitung und Speicherung erlaubt. Das Verwenden und das Bearbeiten stehen unter der Bedingung der Namensnennung. Im Einzelfall kann eine restriktivere Lizenz gelten; dann gelten abweichend von den obigen Nutzungsbedingungen die in der dort genannten Lizenz gewährten Nutzungsrechte.

Documents in HENRY are made available under the Creative Commons License CC BY 4.0, if no other license is applicable. Under CC BY 4.0 commercial use and sharing, remixing, transforming, and building upon the material of the work is permitted. In some cases a different, more restrictive license may apply; if applicable the terms of the restrictive license will be binding.



Numerical Prediction of Ripple Dimensions and Related Roughness for Tidal Environments

B. Putzar¹ and A. Malcherek²

Abstract: *A subgrid-scale model for ripple prediction is presented, which calculates the bed form height and length based on a relaxation algorithm for ripple growth and decrease as a function of the bed shear stress. Herein, equilibrium dimensions are taken into account as well as limits of ripple existence. Based on predicted ripple height and length, the subgrid-scale model calculates the related roughness. The applied approaches and the algorithm are implemented in the morphodynamic numerical model SediMorph. Numerical simulations of a schematic estuary indicate that the presented subgrid-scale model is a step forward to self-calibrating integrated simulation systems.*

Keywords: *bed forms; subgrid-scale model; ripple development; ripple roughness; SediMorph, tidal environment.*

INTRODUCTION

Ripples are bed features with dimensions much smaller than the water depth, generally in the range of a few centimeters. They can grow and decrease depending on the strength of the flow and the sediment parameters. Ripples affect the hydrodynamic roughness of a bed and increase the turbulence production. Their roughness height is higher by order of magnitude compared to that by sediment grains. Therefore, the influence of ripples on the current has to be taken into account when modeling the hydrodynamics. In contrast, hydrodynamic numerical models are adapted to digital terrain models with a resolution of usually one meter or above, where ripple structures are neglected. Their effect on the flow is considered by adjusting the bed roughness manually. But this approach does not consider the development of ripple length and height with time until equilibrium is achieved. Therefore, the influence of these small-scale bed features on the flow should be included in a subgrid-scale model that adapts ripple dimensions to the flow strength and sediment parameters automatically.

This article presents a subgrid-scale model for the numerical prediction of ripple dimensions, namely height and length, and the calculation of the related roughness in tidal flow. It was developed for the morphodynamic numerical model SediMorph (BAW, 2005), which is applied for numerical simulations of coastal waters as well as river

¹ Research Assistant, Institute of Hydro Sciences, University of the German Armed Forces Munich, 85577 Neubiberg, Germany, Email: bert.putzar@unibw.de

² Professor, Institute of Hydro Sciences, University of the German Armed Forces Munich, 85577 Neubiberg, Germany, Email: andreas.malcherek@unibw.de

morphodynamics. The following aspects have to be taken into account in order to develop a sub-grid scale model:

- Ripples are small scale bed forms that develop under certain flow conditions and grain diameters. They can grow until an equilibrium state is reached, where height and length do not change anymore, but get washed out and disappear if the bed shear stress is too high. Ripples have to be distinguished from other bed forms like dunes.
- For the prediction of ripple dimensions a variety of formulae exists for current, waves and combined current-wave flow. In fact, tidal flow can be considered as unidirectional unsteady flow for an appropriate small time period. Therefore, a predictor for equilibrium dimensions under current flow can be applied.
- To predict the development of ripple height and length with time, only a few well-established models for current ripples under steady flow exist. However, development under varying flow or bed form decrease is not yet completely investigated. In this case assumptions have to be made.
- Ripple existence should be limited with the onset of grain motion, an upper threshold considering flow conditions and a range of valid grain diameters. Additionally, these thresholds ensure that ripples can be distinguished from other bed forms.
- Ripple roughness is well investigated and can be calculated as the ripple steepness times the ripple height combined with a coefficient.

The main focus of this article is the description of the formulae applied in the subgrid-scale model for predicting ripple dimensions and the related roughness as well as the implemented algorithm. Results obtained from numerical simulations with SediMorph coupled with TELEMAC-2D for a schematic estuary show the capability of the presented sub-grid scale model.

DESCRIPTION OF THE NUMERICAL MODELS

The Morphological Model SediMorph

SediMorph is a three-dimensional morphological model for graded sediment transport. It solves the bottom evolution equation (Exner equation) and can be coupled with different hydrodynamic models. SediMorph works on a mesh of volume cells. They are generated from the grid of the hydrodynamic model and several vertical bottom layers. A volume cell contains different user defined sediment fractions. For example SediMorph takes into account: initiation of sediment movement according to Shields; bed shear stress by Nikuradse's law; calculation of bed roughness as a sum of grain roughness and form roughness by dunes and ripples, calculation of bed-load transport capacity; user defined active layer thickness and combined current-wave bed shear stress.

The Hydrodynamic Model TELEMAC-2D

TELEMAC-2D is a finite element code and solves the depth-averaged free surface flow equations. The simulation domain is discretised by triangles, which form an unstructured orthogonal mesh. The main results at each node of the computational mesh are the water depth and the depth-averaged velocity components. It can take into account, among others, the following phenomena: propagation of long waves with non-linear effects; intertidal flats; influence of Coriolis force; influence of wind, turbulence and bed shear stress.

Coupling Procedure

SediMorph is coupled with TELEMAC-2D by exchanging required data every time step. At first, the hydrodynamic model calculates the water depth and the mean flow velocity based on the bed roughness and the bed development from the former time step. The hydrodynamic parameters are transmitted to SediMorph. The morphodynamic model computes the new bed roughness and the new bed development using these data and the morphodynamic parameters of the bottom, for example the grain diameter. Afterwards, SediMorph transmits them to TELEMAC-2D for the next time step.

THE SUBGRID SCALE MODEL

Equilibrium Ripple Dimensions

Raudkivi (1997) proposed the following relation for steady flow:

$$\eta_e = 18.16d^{0.097} \quad (1)$$

Here, η_e is the equilibrium height in [mm] that a ripple can reach depending on the grain diameter d in [mm]. The ripple steepness can be calculated according to Raudkivi (1997) as

$$\frac{\eta_e}{\lambda_e} = \frac{0.074}{d^{0.253}} \quad (2)$$

where λ_e is the equilibrium ripple length in [mm] with the grain diameter in [mm].

Relaxation of Ripple Height

Ripple growth for steady flow

Equation (1) and Equation (2) do not take into account the development with time until equilibrium. Based on laboratory data, Coleman et al. (2005) suggest for ripple growth from an initially flat bed the following power law relation:

$$\eta = \eta_e \left(\frac{t}{T_e} \right)^{\gamma_\eta} \quad (3)$$

Here, η is the actual ripple height, t is the actual time of development, T_e is the time to achieve equilibrium and $\gamma_\eta = 0.22D_*^{0.22}$ is a growth factor, where D_* is the dimensionless grain diameter. T_e expressed in terms of the bed shear stress writes:

$$T_e = 2.08 \times 10^8 \left(\frac{\tau_B}{\tau_{cr}} \right)^{-2.42} \frac{d}{u_*} \quad (4)$$

with τ_B the bed shear stress, τ_{cr} the critical shear stress for sediment motion, where a parameterization of the Shields curve is applied to obtain this value. The bed shear velocity is defined as $u_* = \sqrt{\tau_B / \rho}$ with the water density ρ . The bed shear stress is calculated according to Nikuradse's law:

$$\tau_B = \frac{\rho \kappa^2}{\ln\left(\frac{12h}{k_s}\right)^2} u^2 \quad (5)$$

Here, κ is the Karman constant, u is the depth-averaged current velocity vector and h is the water depth. The parameter k_s is Nikuradse's effective roughness coefficient and is calculated after van Rijn (1993) as

$$k_s = k_s^g + k_s^d + k_s^r \quad (6)$$

It is the sum of the grain roughness $k_s^g = 3d$ and the form roughness due to dunes k_s^d and ripples k_s^r . The dimensionless grain diameter is defined as

$$D_* = \left(\frac{(\rho_s - \rho) g}{\rho \nu^2} \right)^{1/3} d$$

where ρ_s is the sediment density, g is the gravity constant and ν^2 is the kinematic viscosity.

The left diagram in Fig. 1 illustrates ripple growth by Equation (3) for $\tau_B / \tau_{cr} = 6$ (blue line) and $\tau_B / \tau_{cr} = 5$ (dashed line) with $d = 2 \times 10^{-4}$ m. The time to achieve equilibrium by Equation (4) for the same grain diameter shows the right diagram of Fig. 1.

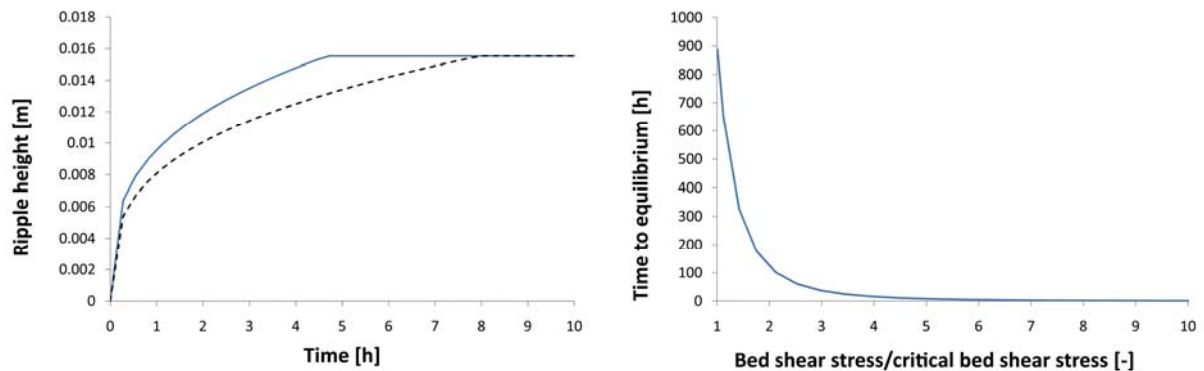


Fig. 1. Ripple growth with time (left) and time to achieve equilibrium dimensions (right) after Coleman et al. (2005)

Ripple growth for unsteady flow

Under varying hydrodynamic and morphodynamic conditions the parameters η_e , T_e and γ_η in Equation (3) change and thus ripple development. Based on preliminary laboratory flume experiments, Coleman et al. (2005) demonstrate that for unsteady flow a modification of the power law gives reasonable results. This idea is adapted for an implementation into the SediMorph model, which illustrates the schematic graph in Fig. 2. Based on Equation (3), the actual ripple height is computed as

$$\eta^{n+1} = \eta_e^{n+1} \left(\frac{t^{n+1}}{T_e^{n+1}} \right)^{\gamma^{n+1}} \quad (7)$$

The index $n+1$ denotes the values calculated by SediMorph for the new time step in the numerical simulation. Note that t^{n+1} is not the simulation time but the actual time of ripple development. t^{n+1} is defined as

$$t^{n+1} = t^n + \Delta t \quad (8)$$

where the index n denotes the previous time step and Δt is the simulation time step. Regarding the power law describing ripple development, t^n is recalculated by identifying $\eta^{n+1} = \eta^n$ in Equation (7). This procedure is marked with a red arrow in Fig. 2. For the previous time of ripple development follows

$$t^n = T_e^{n+1} \left(\frac{\eta^n}{\eta_e^{n+1}} \right)^{1/\gamma^{n+1}} \quad (9)$$

Thus, the ripple height η^{n+1} for a new time step is calculated by Eq. (7), Eq. (8) and Eq. (9).

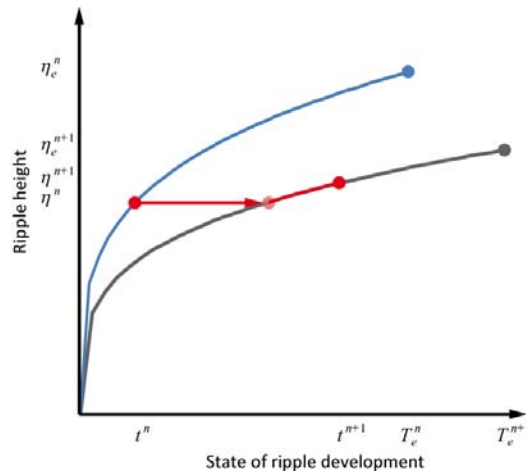


Fig. 2. Schematic representation of ripple growth for unsteady flow

Ripple decrease

Ripple height reduces if for the new time step the equilibrium ripple height is less, the bed shear stress is too high or ripples physically cannot exist. In these cases the course of the function of ripple development is not well-known. Therefore, the approach for dune prediction presented in Malcherek and Putzar (2004) was applied. Thus, ripple height is calculated with the following relaxation formula:

$$\eta^{n+1} = \eta^n + \left(\eta_e^{n+1} - \eta^n \right) \left(\frac{\Delta t}{T_e^{n+1}} \right) \quad (10)$$

Equation (10) is applied for both steady and unsteady flow.

Computing the Ripple Length

The ripple length is computed by the ratio given in Equation (2). This is certainly – in particular for washed out ripples – a simplification of the process. The formula is applied

with regard to ripple roughness with the square of ripple height, and the fact that for high bed shear stress ripples disappear in a small time scale. From Equation (2) it follows

$$\lambda^{n+1} = \eta^{n+1} \frac{d^{0.253}}{0.074} \quad (11)$$

Since the ripple height includes growth and destruction already, a separate relaxation formula for the ripple length is not applied.

Thresholds for Ripple Existence

Ripple develop from a initially flat bed when the effective bed shear stress τ'_B acting on the sediment grains is above the critical shear stress τ_{cr} for sediment motion. Naturally, this is one threshold for their existence. The effective bed shear stress is calculated according to Eq. (5) with Nikuradse's effective roughness coefficient equal to the grain roughness. If the bed shear stress is too high ripples get flatten out and disappear. A threshold is given, amongst others, by Komar and Miller (1975). In dimensional form the formula writes:

$$\tau_{up} = 0.413d^{-0.396}(\rho_s - \rho)gd \quad (11)$$

where τ_{up} is upper threshold of bed shear stress. The grain diameter d has to be in [mm].

Ripple existence is not only limited by the bed shear stress but also by the present sediment fractions. Generally they can appear on a sandy bottom. Therefore, the range of ripple existence is limited by a minimal grain diameter d_{min} and a maximal grain diameter d_{max} . Standard values that can be obtained from literature (Soulsby, 1997, Soulsby and Whitehouse, 2006) are $d_{min} = 6 \times 10^{-5}$ m and $d_{max} = 1 \times 10^{-3}$ m.

Calculation of Ripple Roughness

The effect of ripples on the turbulence production is described in terms of a roughness height, as Equation (6) indicates. According to van Rijn (1993), k_s^r is defined as

$$k_s^r = \alpha_r \gamma \frac{\eta^2}{\lambda} \quad (12)$$

Here, α_r is the ripple roughness coefficient that varies between approximately 8.0 (van Rijn, 1993) and 27.7 (Grant and Madsen, 1982). The parameter γ takes into account if ripples are superposed on dunes ($\gamma = 0.7$) or if only ripples are present ($\gamma = 1.0$). By comparison to grain roughness the roughness by ripples is a multiple larger. Consequently, k_s^r is the determining parameter that influences the hydrodynamic conditions.

Algorithm to predict ripple dimensions and related roughness

The above-mentioned approaches are combined to an algorithm to predict ripple dimensions for unsteady flow and changing bottom sediments. During one simulation time step SediMorph carries out the algorithm for the whole simulation domain.

The first step to predict ripple dimensions is to check the grain diameter of a volume cell. If the value is in the range between the minimal grain diameter d_{min} and the maximal grain diameter d_{max} , ripples can possibly develop. The next step is a distinction by cases for the

effective bed shear stress:

- a) τ'_B is higher than the upper limit τ_{up} of ripple existence, which means ripple decrease. The equilibrium ripple height is set to zero and Equation (10) is applied.
- b) τ'_B is less than the upper limit τ_{up} of ripple existence but higher than the critical bed shear stress τ_{cr} , which means ripple growth or decrease to a certain value. The equilibrium height is calculated by Equation (1) and the time to achieve it according to Equation (4). If the ripple height is less than equilibrium, relaxation Equation (7) is used. In case that it is higher than equilibrium, decrease is calculated according to Equation (10).
- c) τ'_B is less than the critical bed shear stress τ_{cr} and thus the ripple height does not change.

In case that the grain diameter is not valid, ripples can physically not exist. Herein, the effective bed shear stress is not considered. Equation (10) is applied with the aim to reduce ripple height to zero.

After determining the ripple height the ripple length is calculated according to Equation (11) and the related roughness follows from Equation (12).

RESULTS FOR A SCHEMATIC ESTUARY

Simulation Setup

The simulation setup consists of SediMorph coupled with the two-dimensional depth-averaged flow model TELEMAC-2D. The schematic estuary represents a horizontal channel with a length of 50 000 m in x -direction and a width of 1 000 m in y -direction. The grid consists of 14 914 nodes that form 28 370 triangular elements. The bottom was modeled with a grain diameter of $d = 2 \times 10^{-4}$ m for the whole simulation domain and the initial mean water depth was set to 10 m. Liquid boundary conditions were defined in y -direction at the left border of the model for the incoming tide with a wave number $k = 1.4 \times 10^{-5} \text{ m}^{-1}$ and an angular wave frequency of $\omega = 1.4 \times 10^{-4} \text{ s}^{-1}$. The remaining boundaries were treated as solid walls. The simulations with SediMorph coupled with TELEMAC-2D were carried out with a time step of 30 s.

Test Cases

Three simulations were performed to investigate ripple development and the effect of ripple roughness (Table 1). Test case 1 was carried out to simulate only ripple growth. An amplitude of $A = 2.5$ m was used for test case 2 to provoke ripple decrease during a tidal cycle. Test case 3 is similar to test case 1 but with a higher ripple roughness coefficient. Both were compared to investigate the effect of ripple roughness on the tide.

Table 1. Test cases for ripple development and ripple roughness

Test case.	Amplitude [m]	Ripple roughness coefficient [-]
1	1	8

2	2.5	8
3	1	20

Ripple Growth and Ripple Decrease

Fig. 3 illustrates the predicted ripple height for test case 1 after 60 h of simulation. Ripples occur where the bed shear stress is high enough to initiate sediment transport. Equilibrium dimensions are achieved in the area between $x = 0$ m and $x = 32\,000$ m. More close to the reflecting end of the estuary the effective bed shear stress becomes less until sediment transport is not initiated anymore. This leads to a transition area from $x = 32\,000$ m to $x = 33\,000$ m where ripples are present but equilibrium is not achieved. Closer to the end of the estuary they do not emerge since the effective bed shear stress is too low. Fig. 4 shows time profiles for hydrodynamic and morphodynamic parameters. The location $x = 10\,000$ m and $y = 500$ m is marked with an \times in Fig. 3. The ripple increases as soon as sediment transport is initiated after 1 h of simulation time. The development stops when the effective bed shear stress is less than the critical bed shear stress. Therefore, the ripple achieves equilibrium after 12.5 h step-by-step with altering growth and stagnation phases.

The predicted ripple height for test case 2 illustrates Fig. 5. Due to the higher amplitude, the area where ripples occur extends towards the end of the estuary compared to test case 1. The higher effective bed shear stress leads to a different development with time (Fig. 6). After 0.5 h of simulation time ripple height increases and achieves equilibrium 1 h later. But at the end of the tidal cycle the effective bed shear stress reaches the limit for ripple existence, denoted with τ_{up} in Fig. 6, and the ripple height decreases to zero. Later on, growth and decrease alternate. Here, achieving equilibrium conditions and decrease to zero take place within seconds.

Ripple Roughness

The predicted ripple height for test case 3 at a simulation time of 60 h shows Fig. 7. The results are very similar to test case 1, whereby the ripples emerge more away from the end of the estuary and the transition area is less. Fig. 8 shows the time profiles from test case 1 (dotted line) and test case 3 to illustrate the influence of α_r . The comparison of the water level shows that a phase shift exists between both tides. The higher α_r and hence the increased bed shear stress in test case 3 slows down the tide much more than in test case 1. In contrast, the effective bed shear stress is higher with $\alpha_r = 8$ compared to $\alpha_r = 20$. The reason is that the effective bed shear stress takes into account only the flow velocity, the water depth and the grain roughness. Furthermore, equilibrium ripple height is achieved for test case 1 after 12.5 h but for test case 3 already after 8.5 h. It should be remarked that one would expect a faster ripple development with a higher effective bed shear stress. But the opposite is the case, because time to achieve equilibrium is a function of the bed shear stress. The bed roughness including grain and ripple roughness is different between the two cases, as expected. Test case 1 with $\alpha_r = 8$ has a bed roughness when equilibrium ripple height is achieved of $k'_s = 0.0145$ m, whereas this value is more than double with $\alpha_r = 20$.

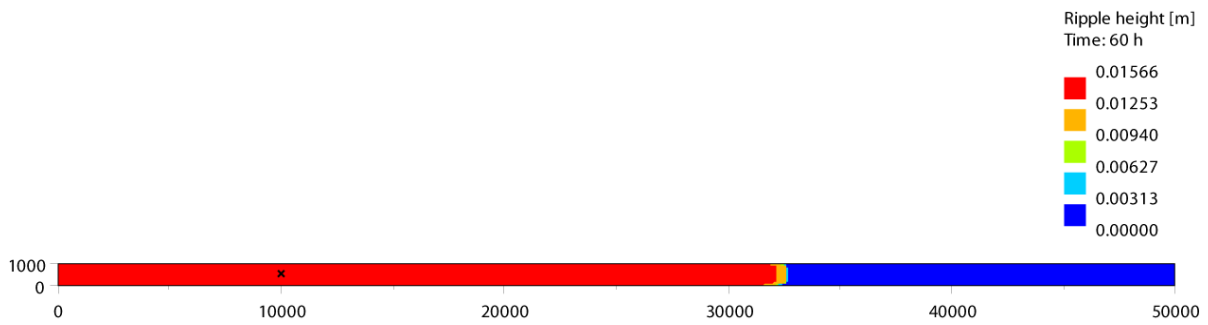


Fig. 3. Predicted ripple height for test case 1 after 60 h of simulation

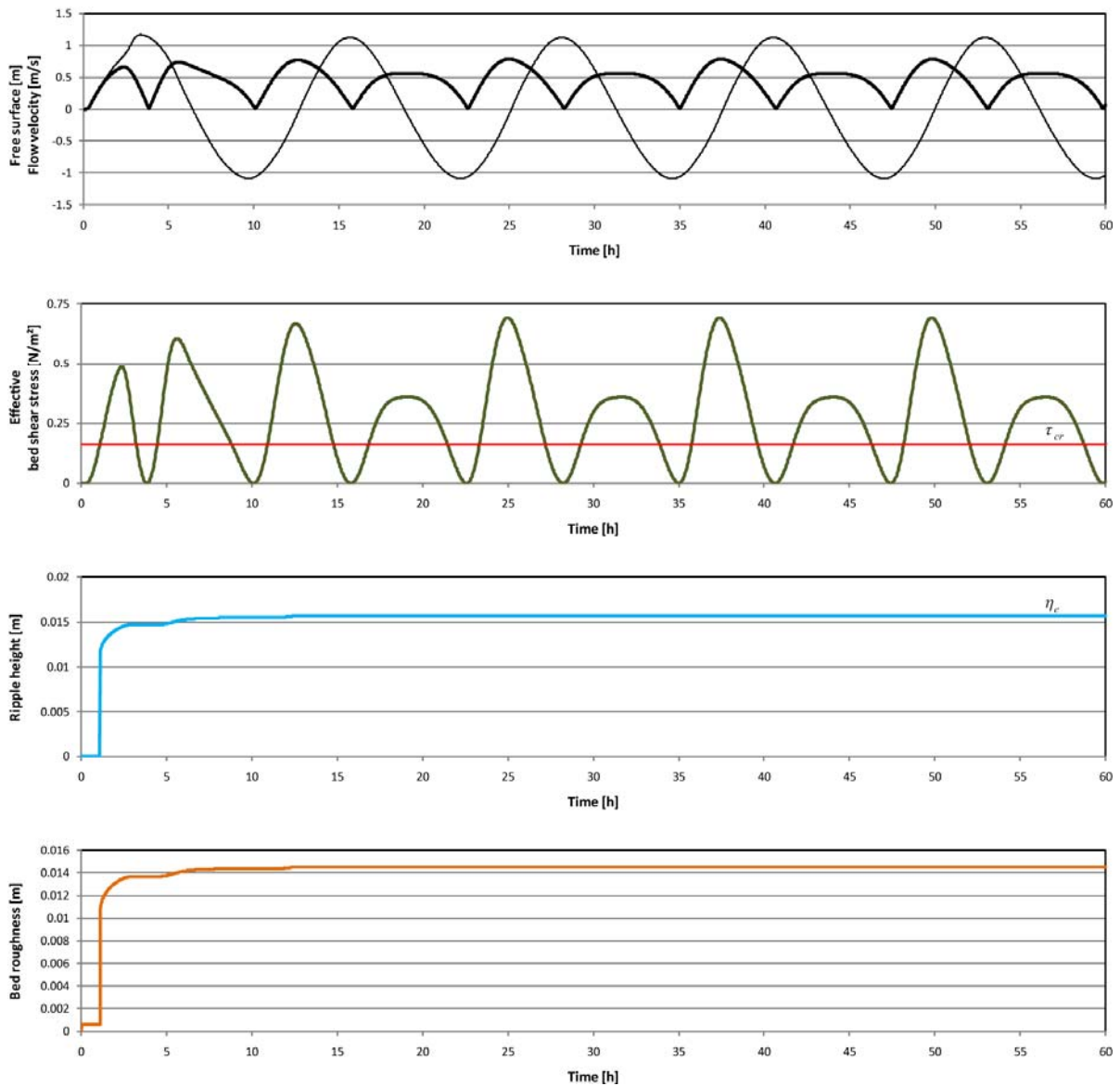


Fig. 4. Time profiles for test case 3 at location $x = 10\,000$ m and $y = 500$ m, which is marked with an \times in Fig 3

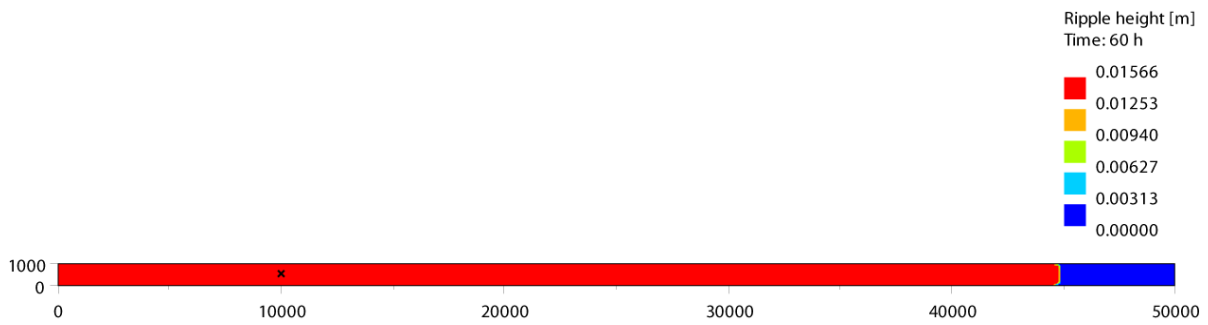


Fig. 5. Predicted ripple height for test case 2 after 60 h of simulation

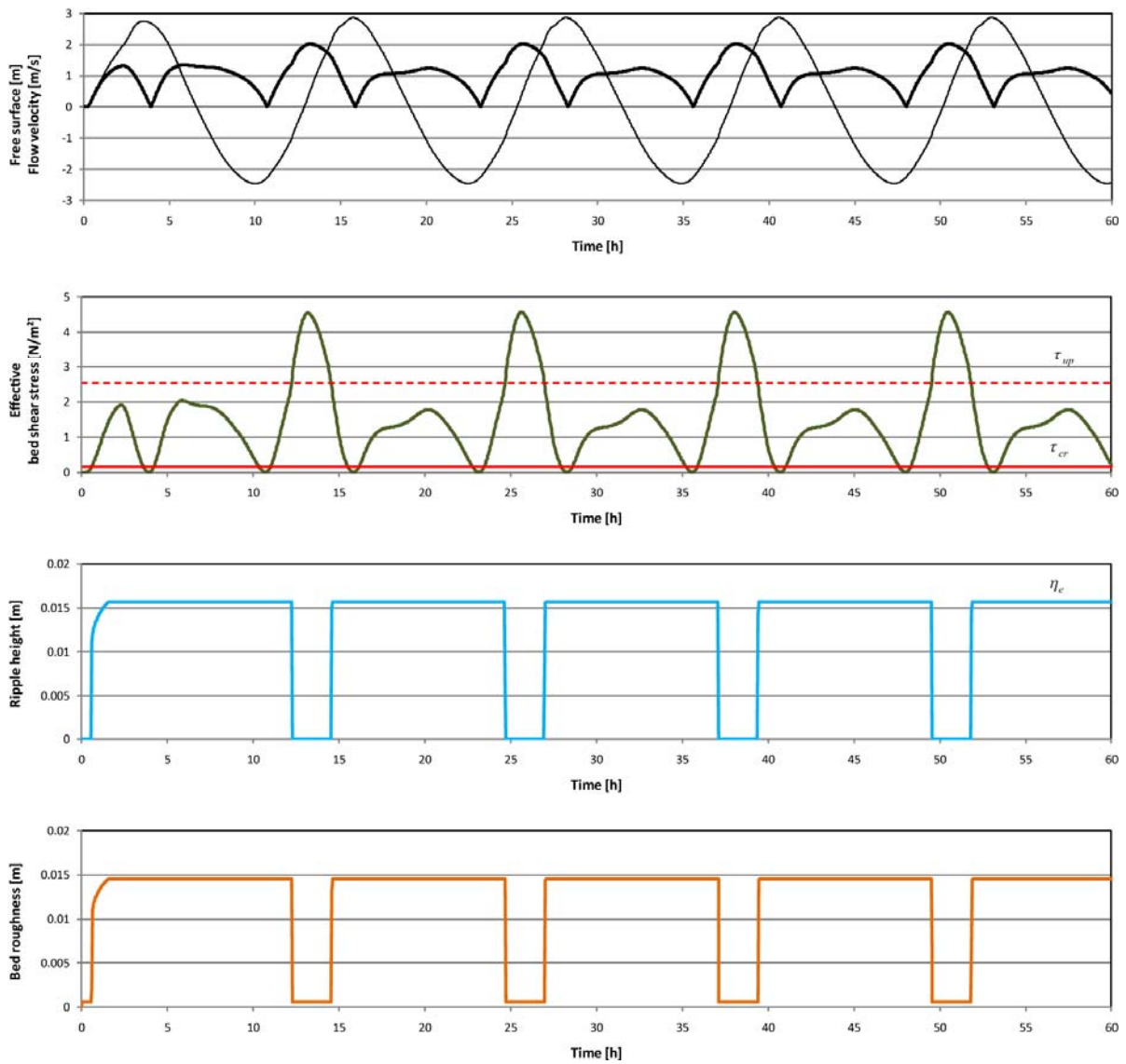


Fig. 6. Time profiles for test case 2 at location $x = 10\,000$ m and $y = 500$ m

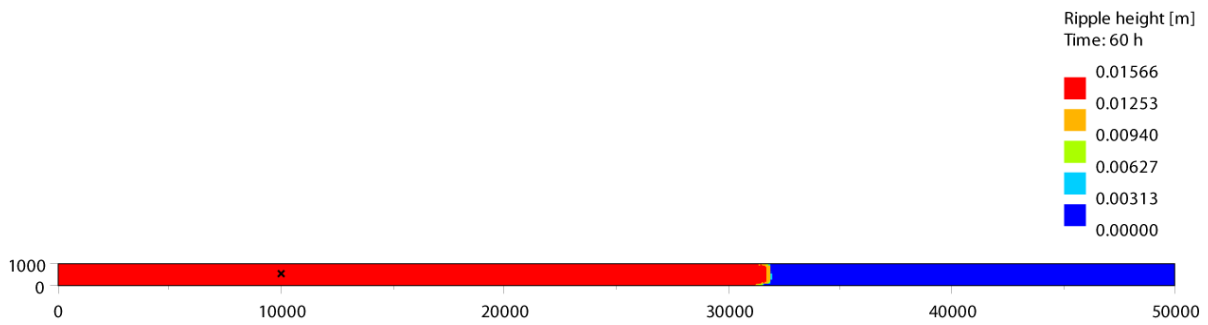


Fig. 7. Predicted ripple height for test case 3 after 60 h of simulation

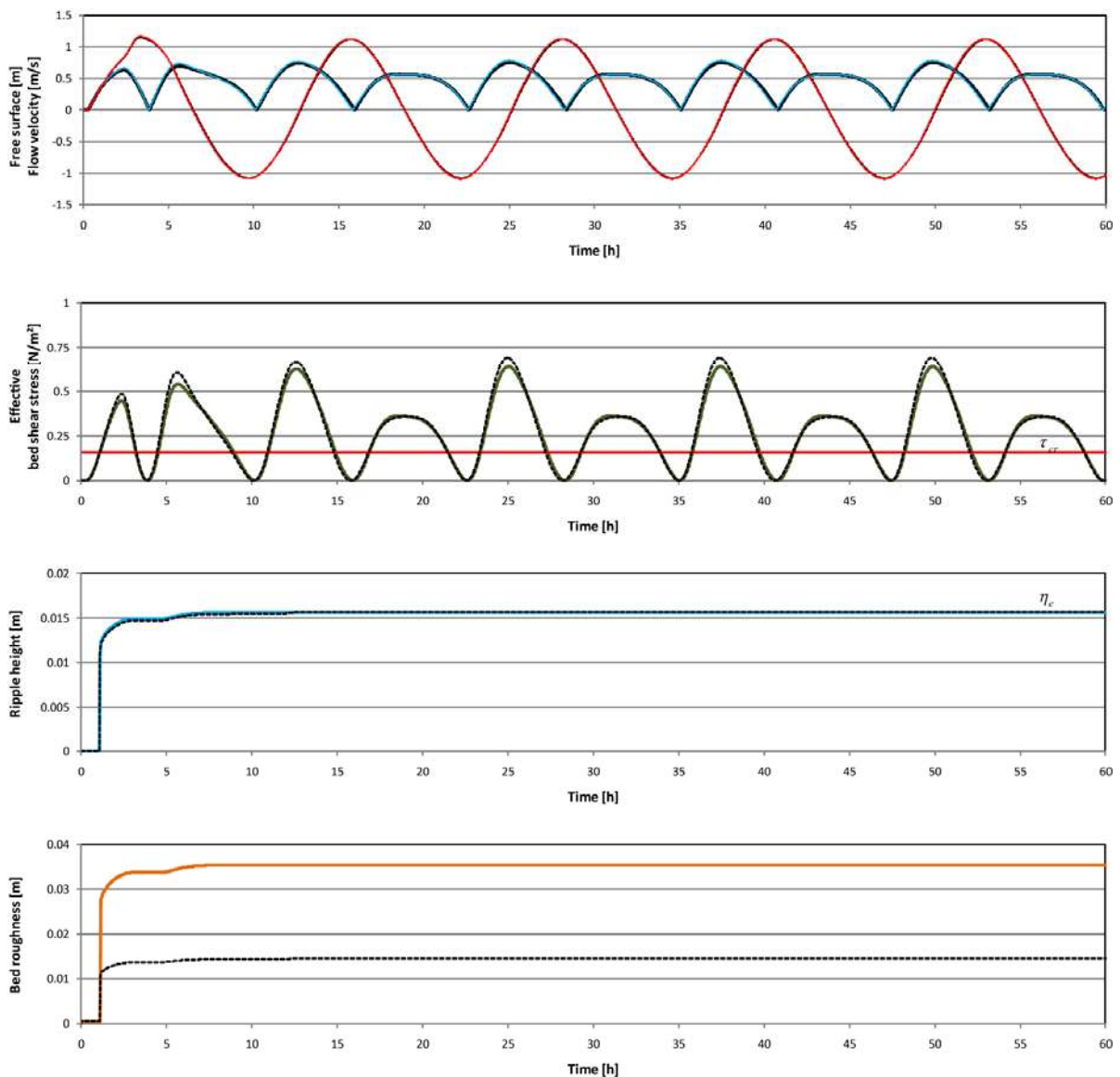


Fig. 8. Comparison of time profiles from test case 1 (dotted line) with results from test case 3 at location $x = 10\,000$ m and $y = 500$ m

CONCLUSIONS

A subgrid-scale model for the numerical prediction of ripple height and length including growth and decrease relaxation algorithms, limits of existence and the calculation of the ripple roughness has been presented. The results of numerical simulations for a schematic estuary shows that ripples can grow and/or decrease during a tidal cycle. The time to achieve equilibrium ranges from a few seconds to several hours. Their effect on the tide is noticeable, whereby the ripple roughness coefficient can have a remarkable influence. For improvement of the proposed subgrid-scale model, it should be applied to real estuaries and compared with field data. The proposed subgrid-scale model applied to coupled morphodynamic-hydrodynamic models provides the opportunity to establish self-calibrating integrated simulation systems.

ACKNOWLEDGEMENTS

The presented work was funded by the Federal Waterways Engineering and Research Institute, Germany. We would like to thank Sandra Wappelhorst for her constructive comments on the manuscript.

REFERENCES

- BAW (2005), *Morphodynamical Module SediMorph – Validation Document*. Federal Waterways Engineering and Research Institute (BAW).
- Coleman, S.E., Zhang, M.H. and Clunie, T. (2005), Sediment-wave development in subcritical water flow, *Journal of Hydraulic Engineering*, 131 (2), 106-111.
- Grant, W. D. and Madsen, O. S. (1982), Movable bed roughness in unsteady oscillatory flow, *Journal of Geophysical Research*, 87 (C1), 469-481.
- Hervouet, J.M. and Bates, P. (2000), The TELEMAC Modelling System. Special issue of *Hydrological Processes*, 14, 2207-2208
- Komar, P.D. and Miller, M.C. (1975), The initiation of oscillatory ripple marks and the development of plane bed at high shear stresses under waves, *Journal of Sedimentary Petrology*, 45, 697-703.
- Malcherek, A. and Putzar, B. (2004), The Prediction of Dunes and Their Related Roughness in Estuarine Morphological Models, *Proceedings of the 8th Int. Conference on Estuarine and Coastal Modeling*, Monterey, California, 839-851.
- Raudkivi, A.J. (1997), Ripples on stream bed, *Journal of Hydraulic Engineering*, 123 (1), 58-64.
- Rijn, L. C. van (1993), *Principles of Sediment Transport in Rivers, Estuaries and Coastal Seas*, Aqua Publications, Amsterdam.
- Soulsby, R. (1997), *Dynamics of Marine Sands*, Thomas Telford Publications, London.
- Soulsby, R.L. and Whitehouse, R.J.S. (2006), Prediction of ripple geometry for acoustic response and hydrodynamic roughness applications, *Coastal Engineering 2006 - Proceedings of the 30th International Conference*, Ed. J. McKee Smith, 2415-2427.